Tunable UCST thermoresponsive copolymers based on natural glycyrrhetinic acid

Yiran Zhao, Jingyao Ma, Xia Yu, Min-Hui Li, Jun Hu

Communication

Tunable UCST thermoresponsive copolymers based on natural glycyrrhetinic acid

Yiran Zhao[a], Jingyao Ma[a], Xia Yu[a], Min-hui Li[a,b,*], Jun Hu[a,*]

[a]*Beijing Advanced Innovation Center for Soft Matter Science and Engineering, Beijing University of Chemical Technology, Beijing 100029, China*
[b]*Institut de Recherche de Chimie Paris, Chimie ParisTech, PSL Research University, CNRS, Paris 75005, France*

ARTICLE INFO

Article history:
Received
Received in revised form
Accepted
Available online

Keywords:
thermo-responsive polymer
UCST
glycyrrhetinic acid
natural product
cyclodextrin

ABSTRACT

Water-soluble thermoresponsive polymers present either upper critical solution temperature (UCST) or lower critical solution temperature (LCST) depending on the location of their miscibility range with water at high temperatures or at low temperatures. Compared with LCST polymers, the water-soluble UCST polymers are still less explored until now. In this work three copolymers of P(AAm-*co*-GAA) were synthesized by copolymerizing two acrylamide monomers, acrylamide (AAm) and acrylamide functionalized with natural glycyrrhetinic acid (GAA), using reversible addition-fragmentation chain transfer (RAFT) polymerization. These copolymers exhibited the typical UCST thermoresponsive behavior, and their phase transition temperatures could be easily tuned to around 37 ºC for potential biological applications. Moreover, the UCST of P(AAm-*co*-GAA) can be adjusted not only by the content of glycyrrhetinic acid (GA) and polymer concentrations, but also by the host-guest interactions between GA and cyclodextrins (*β*- and *γ*-CD). The suitable value of UCST and the biocompatible nature of GA and CDs may endow these copolymers with practical applications in biomedical chemistry.

Water-soluble thermoresponsive polymers have been widely studied in polymer and material science due to the drastic hydrophilicity/hydrophobicity transformation upon changes of temperature [1,2]. They can be divided into lower critical solution temperature (LCST)-type and upper critical solution temperature (UCST)-type, depending on the drop of miscibility at low temperatures or at high temperatures [3]. After the discovery of LCST behavior of poly(N-isopropylacrylamide) by Heskins and co-workers in 1968 [4], numerous water-soluble LCST polymers have been reported [5,6]. Compared with LCST polymers, the UCST polymers are less explored since they were discovered later and the number of examples was still limited [7,8]. The UCST behavior stems from either Coulomb interactions (the effect of amphoteric ions) or hydrogen bonding, namely C-UCST or HB-UCST, respectively [9]. As C-UCST behavior depends heavily on ionic strength, type of ion and pH value, the potentials of C-UCST polymers are restricted because in most applications mild ionic strength is required [9,10]. Thus, HB-UCST polymers which are less sensitive to electrolytes would be more suitable for preparing thermosensitive materials.

In 2012, Seuring and co-workers copolymerized acrylamide and acrylonitrile to afford poly(acrylamide-*co*-acrylonitrile) with the typical UCST behavior in water [11]. Later, researchers used additional comonomers to copolymerize with acrylamide (AAm) and acrylonitrile (AN), and applied them in various fields [12-14]. For example, Zhao and co-workers reported an ultrasensitive pH-induced water-soluble switch by incorporating either acrylic acid or 4-vinylpyridine comonomers in the random copolymer of acrylamide and acrylonitrile [12]. Sukhishvili and co-workers have synthesized a HB-UCST block copolymer, poly(acrylamide-*co*-acrylonitrile)-*b*-polyvinylpyrrolidone, and prepared its self-assembled films with thermoresponsive properties [13]. Apparently, incorporating a suitable hydrophobic unit into the water-soluble polymer chain would be an effective strategy to obtain HB-UCST polymers.

Glycyrrhetinic acid (GA) is one of the physiologically natural triterpenoids in vivo and plays key roles in a variety of remarkable biological activities [15]. In addition, GA has the rigid hydrophobic scaffold, great biocompatibility, multiple reactive sites and chiral centers. These characteristics can be used to make low molecular weight gels [16,17], supramolecular chiral structures [18], and functional polymers [19,20]. In our previous works, GA has been incorporated into LCST-based polymers, "necklace"-like polypseudorotaxanes, and self-healable hydrogels [21-23]. In this work, we proposed to take advantage of the hydrophobic backbone of GA to construct new biocompatible HB-UCST polymers. Three copolymers of P(AAm-*co*-GAA-x%) (x = 2, 3, 4) were designed and

∗ Corresponding author.
E-mail address: jhu@mail.buct.edu.cn (J. Hu), min-hui.li@chimieparistech.psl.eu (M. Li).

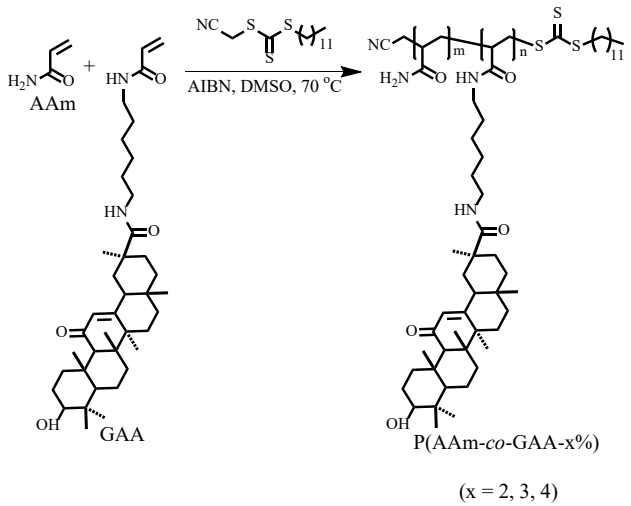

Scheme 1. Illustration of copolymerization of natural glycyrrhetinic acid-derived acrylamide (GAA) with acrylamide (AAm).

synthesized (Scheme 1), where an acrylamide monomer bearing GA (GAA) copolymerized with acrylamide by reversible addition-fragmentation chain transfer (RAFT) polymerization (synthetic details see Supporting Information). The results showed that P(AAm-*co*-GAA) exhibited the typical HB-UCST behavior with a phase transition temperature around 37 °C. Moreover, their thermoresponsive behavior can be adjusted not only by the content of GA and polymer concentrations, but also the host-guest interactions between GA and *β*-/*γ*-cyclodextrin (CD). The suitable UCST and the biocompatible nature of GA and CDs may allow these copolymers to be useful in biomedical field.

The copolymers with different molar ratios of GAA and AAm were characterized by size exclusion chromatography (SEC) and ^{1}H NMR spectra (Fig. S1 and S2). The ^{1}H NMR spectra of P(AAm-*co*-GAA-x%) (x = 2, 3, 4) displayed the characteristic peaks corresponding to protons carried by GA (δ = 5.49 ppm, assigned to H_a; 1.35, 1.05, 1.02, 0.92, 0.74, 0.71 ppm, assigned to methyl groups), and the content of GA unit in copolymers was calculated from the proton integration ratio between the peak at 5.49 ppm (H_a) versus backbone protons at 2.13 ppm (H_b, H_c) (Fig. S2). Meanwhile, in order to explore the UCST mechanism, two control copolymers, P(AAm-*co*-HAA-3%) and P(MMA-*co*-GAA-3%), were synthesized as shown in Scheme S1 (synthetic details see Supporting Information). Compared with P(AAm-*co*-GAA-3%), the rigid hydrophobic backbone of GA was replaced with a flexible alkyl chain (15-hydroxypentadecanoic acid, HA) in P(AAm-*co*-HAA-3%), while the hydrophilic AAm was substituted by the H-bonding-free methyl methacrylate (MMA) in P(MMA-*co*-GAA-3%). All the information on compositions of these copolymers was illustrated in Table 1.

The thermal response of polymer aqueous solutions was recorded by UV-Vis spectrometer. As shown in Fig. 1A, the phase transition with a UCST of 32 °C of P(AAm-*co*-GAA-3%) at the concentration of 15 mg/mL was observed upon cooling, strongly revealing the UCST behavior of P(AAm-*co*-GAA-3%) in the range from 10 to 60 °C. At a high temperature of 40 °C, a clear solution formed, while at 20 °C it appeared a cloudy suspension (inset in Fig. 1A). Either increasing or decreasing the molar fraction of GAA to 4 mol% or 2 mol% led to the UCST higher than 60 °C or lower than 10 °C. It was because P(AAm-*co*-GAA-2%) was less hydrophobic in comparison with P(AAm-*co*-GAA-3%), while P(AAm-*co*-GAA-4%) was more hydrophobic. With increasing the GA content, the hydration shell of hydrophobic segments of copolymers became more ordered [24]. In this case, a higher temperature was needed to dissolve the aggregates, i.e. a high phase transition temperature. Apparently, the content of hydrophobic GA unit had a significant effect on UCST behavior. Notably, compared with the reported P(AAm-*co*-AN) which exhibited the UCST behavior only when AN content was more than 10 mol% [11], P(AAm-*co*-GAA) would show UCST behavior with the content of GAA as low as 3 mol%. Such difference was mainly due to GAA had a larger hydrophobic rigid backbone than AN moiety.

In addition, there was a significant concentration dependence of UCST. As shown in Fig. 1B, the UCST of P(AAm-*co*-GAA-3%) decreased from 32, to 21 °C, and to < 10 °C when the concentration decreased from 15, to 10 and to 5 mg/mL. This observation can be explained by the strong inter- and intra-molecular H-bonding between polymer chains at the high concentration, as solubilizing copolymers required the disruption of polymer-polymer interactions by heat in favor of polymer-water interactions.

Moreover, this phase transition was reversible in multiple heating-cooling processes (3 cycles, Fig. 1C), indicating that no chemical change happened in the system. It should be noted that there was a certain hysteresis which was attributed to the chain mobility of P(AAm-*co*-GAA-3%) below or above UCST. Above UCST, GA pendants was involved in the aggregates companied by the weakening of inter- and intra-molecular H-bonding, and these aggregates were stable enough to delay the generation of large clusters during the cooling process, thus causing the hysteresis [11]. Besides, the thermoresponsive experiments of control polymers (P(AAm-*co*-HAA-3%) and P(MMA-*co*-GAA-3%) were performed. As shown in Fig. S3, the transmittance of P(AAm-*co*-HAA-3%) aqueous solution maintained approximate 90% within the test temperature range from 10 to 60 °C, and did not exhibit any UCST property. It strongly revealed that only the rigid scaffold of GA can afford the suitable face-to-face hydrophobic stacking effect in this UCST-type phase transition,

Table 1
Characteristics of these copolymers.

Copolymer	GAA or HAA in feed (mol%)	GAA or HAA in product (mol%)[a]	M_n (g/mol)	$Đ$[b]	UCST (°C)[c]
P(AAm-*co*-GAA-2%)	2.0	1.7	17100[b]	2.07	< 10
P(AAm-*co*-GAA-3%)	3.0	2.5	12700[b]	1.77	32
P(AAm-*co*-GAA-4%)	4.0	3.6	6700[b]	2.19	> 60
P(AAm-*co*-HAA-3%)	3.0	2.4	14800[a]	-	-
P(MMA-*co*-GAA-3%)	3.0	2.6	11800[b]	1.23	-

[a]Determined by ^{1}H NMR spectrum; [b]determined by SEC spectrum; [c]determined by UV-Vis spectrum at the concentration of 15 mg/mL.

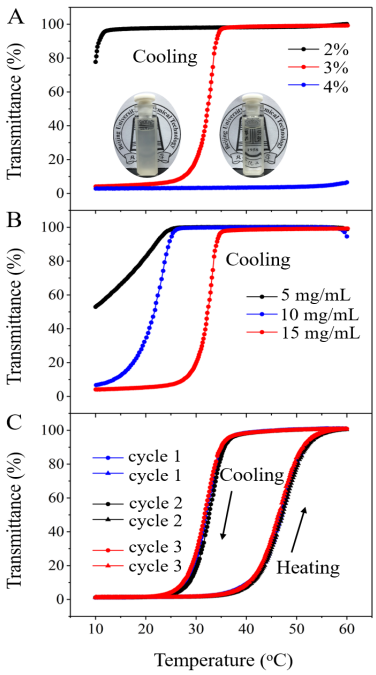

Fig. 1. Transmittance of the copolymer aqueous solutions as a function of temperature at a wavelength of 450 nm: (A) with different GAA molar ratios of P(AAm-*co*-GAA-x%) (x = 2, 3, 4) under the concentration of 15 mg/mL. Inset: digital photos of P(AAm-*co*-GAA-3%) at 20 °C (left) and 40 °C (right); (B) at different concentrations of P(AAm-*co*-GAA-3%); (C) the aqueous solution of P(AAm-*co*-GAA-3%) with three cooling-heating cycles at the concentration of 15 mg/mL. Cooling and heating rate is 1.0 °C/min.

since the better mobility of the flexible alkyl chain HA tended to form chain entanglements, thus restricting their supramolecular complexation and resulting in no phase transition [24]. For the H-bonding-free P(MMA-*co*-GAA-3%) aqueous solution, its transmittance was less than 1% from 10 to 60 °C, and no UCST behavior was observed, which indicated that the H-bonding monomer AAm was necessary in this UCST system. Based on the results of control experiments, it was proposed that the synergistic effect of inter- and intra-molecular H-bonding of amide groups and the face-to-face hydrophobic stacking of GA moieties promoted the appearance of UCST phenomenon.

More evidences for the UCST behavior of P(AAm-*co*-GAA-3%) were revealed by dynamic light scattering (DLS) measurements, ^{1}H NMR spectra, and transmission electron microscope (TEM) images. As shown in Fig. 2A, the average particle size of P(AAm-*co*-GAA-3%) in water was approximately 30 nm when the temperature was above 40 °C. Once cooling to 20 °C, some large clusters around 1000 nm appeared rapidly. With the continuous decrease of temperature, more and more large clusters formed with the disappearance of small particles, eventually a turbid solution was obtained at 10 °C. These observations can be further confirmed by TEM images, where the small particles around 40 nm were observed at 40 °C (Fig. 2B), while only irregular large precipitates were observed at 20 °C (Fig. 2C). The temperature-dependent ^{1}H NMR experiments showed that all proton peaks of P(AAm-*co*-GAA-3%) in D_2O became broad with the decrease of temperature from 60 to 25 °C, especially the signals of methyl groups on GA (Fig.

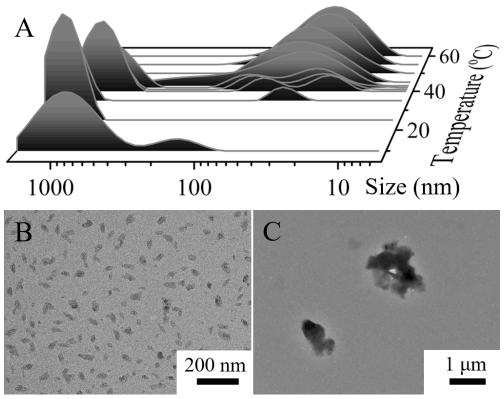

Fig. 2. (A) Temperature-dependent size variation of P(AAm-*co*-GAA-3%) aqueous solution. TEM images of P(AAm-*co*-GAA-3%) aqueous solution at (B) 40 °C and (C) 20 °C without stain. Concentration is 15 mg/mL.

S4). The explanation was that at high temperature above UCST the GA side chain was exposed to D_2O and presented good mobility, while at low temperature the intra- and inter-molecular H-bonding caused the GA side chain to be wrapped by polyacrylamide chains and to be less mobile. In conclusion, all results from the experiments of ^{1}H NMR, UV-Vis, DLS and TEM were totally consistent.

Our previous work has revealed that GA (molecular size 0.58−0.60 nm) could form the host-guest inclusion complex with *β*-cyclodextrin (*β*-CD) (cavity diameter 0.60−0.65 nm, binding constant K_a = 1.59 × 10^3 M^{-1}) and with *γ*-cyclodextrin (*γ*-CD) (cavity diameter 0.70−0.83 nm, K_a = 4.41 × 10^5 M^{-1}), except *α*-CD (cavity diameter ~0.47 nm) [22,25]. Inspired by the size-match effect between GA and CDs, we studied here the role of CDs in adjusting the USCT behavior of P(AAm-*co*-GAA-3%). The ^{1}H NMR spectrum was firstly used to confirm the complexation of CDs with GA units in P(AAm-*co*-GAA-3%). As shown in Fig. S5, no signal of GA was observed in D_2O at room temperature because of the poor solubility of P(AAm-*co*-GAA-3%). Upon addition of *β*-CD and *γ*-CD, respectively, the characteristic methyl peaks of GA units appeared, while no

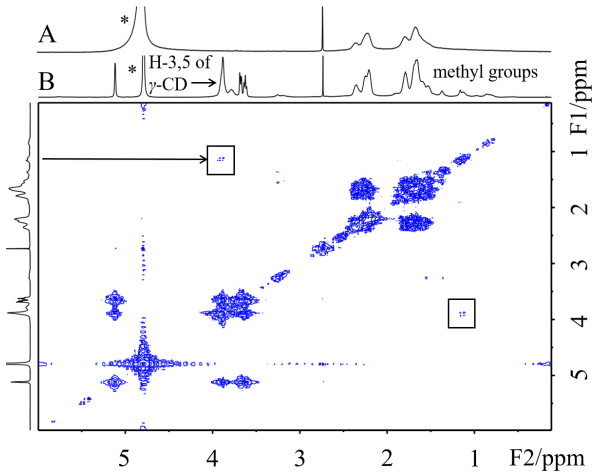

Fig. 3. (A) ^{1}H NMR spectrum of P(AAm-*co*-GAA-3%) in D_2O (400 MHz, 25 °C, concentration = 15 mg/mL). (B) 2D NOESY ^{1}H NMR spectrum of P(AAm-*co*-GAA-3%) with *γ*-CD in D_2O (600 MHz, 25 °C, [GA]/[*γ*-CD] = 1:1, concentration = 15 mg/mL). "*" means residual H signal in D_2O.

change was observed upon α-CD addition. Moreover, cross correlation signals were observed clearly in 2D NOESY ^{1}H NMR spectrum (rectangles in Fig. 3 and S6), indicating the close contact between GA methyl protons and β-/γ-CD protons (limit of detection for NOE signal: <5 Å). As in the aqueous environment GA and CD were phase-separated, these cross-correlation signals were attributed to the formation of inclusion complex by positioning GA moiety in the cavity of β-/γ-CD.

In the UV-Vis absorption experiments, α-CD had no effect on the UCST behavior because of its small cavity diameter (Fig. 4A) [25]. The change in the curve shape was mainly due to the H-bonding between hydroxyl groups of α-CD and amide groups in polymers. In contrast, the significant changes were observed both for β-CD and γ-CD. In the presence of β-CD, P(AAm-*co*-GAA-3%) still exhibited the UCST property, while its UCST decreased gradually with the increase of molar ratio of [β-CD]/[GA] (Fig. 4B). When [β-CD]/[GA] increased from 0 to 0.03, 0.06, and 0.10, the UCST decreased from 32 to 27, 24, and 19 °C. Such results were mainly due to the hydrophilic exterior of β-CD, which enhanced the hydrophilicity of polymers, thus resulting in the decrease of UCST. Note that the UCST was extremely sensitive to the molar ratio of [β-CD]/[GA]. As shown in Fig. 4B, a tiny increase of concentration ratio from 0 to 0.03 would result in a decrease of 5 °C in UCST. This was totally different from the behavior of LCST polymers in the presence of β-CD as reported in our previous work, where an increase of [β-CD]/[GA] ratio from 0 to 5 only resulted in an increase of 13 °C for the cloud point [21]. As γ-CD had a stronger binding ability with GA and a better hydrophilicity compared with β-CD, it was more effective in regulating the USCT behavior of P(AAm-*co*-GAA-3%). As shown in Fig. 4C, a decrease of 13 °C for UCST was achieved upon addition of 0.03 equiv. γ-CD, and the UCST decreased further to lower than 10 °C when 0.06 equiv. of γ-CD was added. Obviously, the host-guest interactions between GA and β/γ-CD would be an effective strategy to regulate the UCST behavior of polymers, and the UCST of P(AAm-*co*-GAA-3%) was more sensitive to γ-CD than to β-CD.

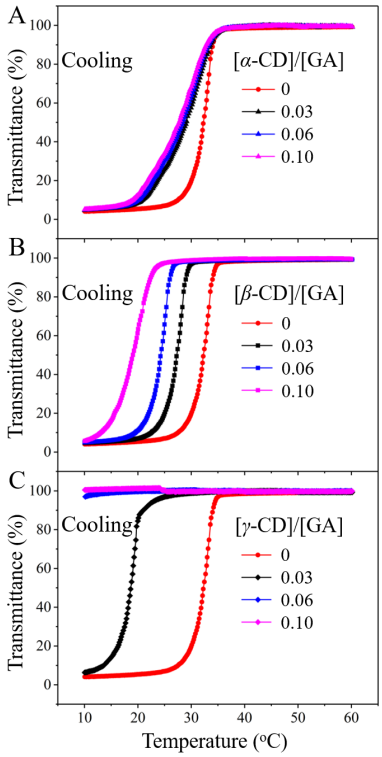

Fig. 4. Transmittance of P(AAm-*co*-GAA-3%) aqueous solution as a function of temperature at a wavelength of 450 nm in the presence of (A) α-CD, (B) β-CD, and (C) γ-CD. Cooling rate is 1.0 °C/min. Concentration is 15 mg/mL.

In summary, by incorporating acrylamide monomer functionalized by natural glycyrrhetinic acid into the polyacrylamide chains, three copolymers of P(AAm-*co*-GAA-x%) (x = 2, 3, 4) were synthesized, which exhibited the typical HB-UCST behavior in water promoted by the synergistic effect of the intra- and inter-molecular H-bonding of amide groups and the face-to-face hydrophobic stacking of GA units. Their phase transition temperatures could be easily adjusted to the temperature range from below 10 to above 40 °C by the GA content and polymer concentrations. Moreover, the UCST can be further tuned by β-CD or γ-CD effectively due to host-guest interactions between GA and CDs. The suitable UCST ranges and the biocompatible features of GA and CDs are particularly interesting for thermoresponsive polymers applied in biomedical field.

Acknowledgment

This work is supported by National Key R&D Program of China (no. 2017YFD0200302) and NSFC (no. 21604085).

References

[1] N. Vanparijs, L. Nuhn, B. G. De Geest, Chem. Soc. Rev. 45 (2017) 1193-1239.
[2] W. Sun, Z. An, P. Wu, Macromolecules 50 (2017) 2175-2182.
[3] J. Niskanen, H. Tenhu, Polym. Chem. 8 (2017) 220-232.
[4] M. Heskins, J. E. Guillet, J. Macromol. Sci., Part A: Chem. 2 (1968) 1441-1455.
[5] H. Zhang, T. Marmin, É. Cuierrier, et al., Polym. Chem. 6 (2015) 6644-6650.
[6] J. Hunold, T. Wolf, F. R Wurm, D. Hinderberger, Chem. Commun. 55 (2019) 3414-3417.
[7] S. Kuroyanagi, N. Shimada, S. Fujii, et al., J. Am. Chem. Soc. 141 (2019) 1261-1268.
[8] T. Maji, S. Banerjee, Y. Biswas, T. K. Mandal, Macromolecules 48 (2015) 4957-4966.
[9] J. Seuring, S. Agarwal, ACS Macro Lett. 2 (2013) 597-600.
[10] J. Seuring, S. Agarwal, Macromol. Rapid Commun. 33 (2012) 1898-1920.
[11] J. Seuring, S. Agarwal, Macromolecules 45 (2012) 3910-3918.
[12] H. Zhang, S. Guo, W. Fan, Y. Zhao, Macromolecules 49 (2016) 1424-1433.
[13] A. Palanisamy, S. A. Sukhishvili, Macromolecules 51 (2018) 3467-3476.
[14] G. Huang, H. Li, S. T. Feng, et al., Macromol. Chem. Phys. 216 (2015) 1014-1023.
[15] O. V. Salomatina, A. V. Markov, E. B. Logashenko, et al., Bioorg. Med. Chem. 22 (2014) 585-593.
[16] A. Saha, J. Adamcik, S. Bolisetty, S. Handschin, R. Mezzenga, Angew. Chem. Int. Ed. 54 (2015) 5408-5412.
[17] B. G. Bag, R. Majumdar, RSC Adv. 2 (2012) 8626-8626.
[18] Y. Gao, J. Hao, J. Wu, et al., Nanoscale 7 (2015) 13568-13575.
[19] M. Zhang, H. Cheng, Z. Gong, et al., Adv. Funct. Mater. 27 (2017) 1703932-1703944.
[20] Q. Tian, C. Zhang, X. Wang, et al., Biomaterials 31 (2010) 4748-4756.
[21] J. Hao, Y. Gao, Y. Li, et al., Chem. Asian. J. 12 (2017) 2231-2236.
[22] J. Hao, Y. Gao, C. Zheng, et al., ACS Macro Lett. 7 (2018) 1131-1137.
[23] Y. Li, J. Li, X. Zhao, et al., Chem. Eur. J. 22 (2016) 18435-18441.
[24] C. Zhao, Z. Ma, X. X. Zhu, Prog. Polym. Sci. 90 (2019) 269-291.
[25] A. Harada, Y. Takashima, M. Nakahata, Acc. Chem. Res. 47 (2014) 2128-2140.

Supporting Information

Tunable UCST thermoresponsive copolymers based on natural glycyrrhetinic acid

Yiran Zhao[a], Jingyao Ma[a], Xia Yu[a], Min-Hui Li[a,b,*], Jun Hu[a,*]

[a]Beijing Advanced Innovation Center for Soft Matter Science and Engineering, Beijing University of Chemical Technology, Beijing 100029, China

[b]Chimie ParisTech, PSL University Paris, CNRS, Institut de Recherche de ChimieParis, 75005 Paris, France

Email: jhu@mail.buct.edu.cn; min-hui.li@chimieparistech.psl.eu

Table of Contents

Materials. Glycyrrhetinic acid (GA), 15-hydroxypentadecanoic acid (HA), N-hydroxysuccinimide (NHS), N,N'-dicyclohexylcarbodiimide (DCC), 1,6-hexylenediamine, acryloyl chloride, triethylamine, potassium *tert*-butoxide, 1-dodecanethiol, carbon disulfide, chloroacetonitrile, *α*-/*β*-/*γ*-cyclodextrin (CD) and other reagents were local commercial products and used as received. 2,2'-Azobis(isobutyronitrile) (AIBN) was recrystallized twice from methanol. Acrylamide (AAm) was recrystallized twice from chloroform and stored at -10 °C. Methyl methacrylate (MMA) was passed through a neutral alumina column to remove the inhibitor and stored at -10 °C. Milli-Q water was used throughout the experiments.

Methods. NMR spectra in $CDCl_3$, $CDCl_3/CD_3OD$, d_6-DMSO or D_2O were recorded on Bruker AVANCE III HD spectrometer operating at 400 MHz for $^1H/^{13}C$ at 25 °C. Temperature-dependent ^1H NMR spectra in D_2O were recorded on Bruker AV600 spectrometer operating at 600 MHz upon cooling from 60 to 25 °C. 2D NOESY ^1H NMR spectra were recorded on Bruker AV600 spectrometer operating at 600 MHz in D_2O at 25 °C.

Electrospray ionization mass spectroscopy (ESI-MS) was analyzed on a Bruker ESQUIRE-LC spectrometer in positive mode. High-resolution mass spectrometry (HRMS) was measured by Ultra High Definition (UHD) Accurate-Mass Q-TOF LC-MS in positive mode.

Molecular weight and molecular weight distribution (M_w/M_n) of P(AAm-*co*-GAA-x%) (x = 2, 3, 4) were determined on a gel permeation chromatograph (PL-GPC 50 Plus, Varian) with DMSO containing 0.05 M LiBr as eluent (flow rate: 0.6 mL/min, at 50 °C) against dextran standards. Molecular weight and M_w/M_n of P(MMA-*co*-GAA-3%) were analyzed by using a Shimadzu gel permeation chromatography system equipped with a SIL-20A autosampler, a refractive index detector, three Shodex KF-805L columns (8 × 300 mm^2, 10 μm, 5000 Å), and one Shodex KF-801 column (8 × 300 mm^2, 6 μm, 50 Å) using DMAC containing 0.05 M LiCl as the eluent (flow rate: 1.0 mL/min, at 50 °C) against polystyrene standards.

Phase transition temperature was determined on a Jasco ETC-505S UV-vis spectrophotometer equipped with a Jasco ETC-505T temperature controller. Polymer aqueous solutions were normally heated and cooled at a rate of 1.0 °C/min. The phase transition temperature was taken as the 50% transmittance change at 450 nm.

Dynamic light scattering (DLS) measurements were performed at different temperatures using Zetasizer Nano-ZS90 instrument equipped with a monochromatic coherent He–Ne laser (633 nm).

Transmission electron microscopy (TEM) images were obtained using Hitachi HT7700 with a maximum accelerating voltage of 120 kV. The samples were prepared as follows: 1) for the sample at 20 °C, a drop of polymer solution (15 mg/mL) at 20 °C was dropped on 300-mesh carbon-coated copper grids which was placed on a hot stage of 20 °C, followed by the removal of water through filter paper after 30 s; 2) for the sample at 40 °C, a drop of polymer solution (15 mg/mL) at 40 °C was dropped on 300-mesh carbon-coated copper grids which was placed on a hot stage of 40 °C, followed by the removal of water through filter paper after 30 s.

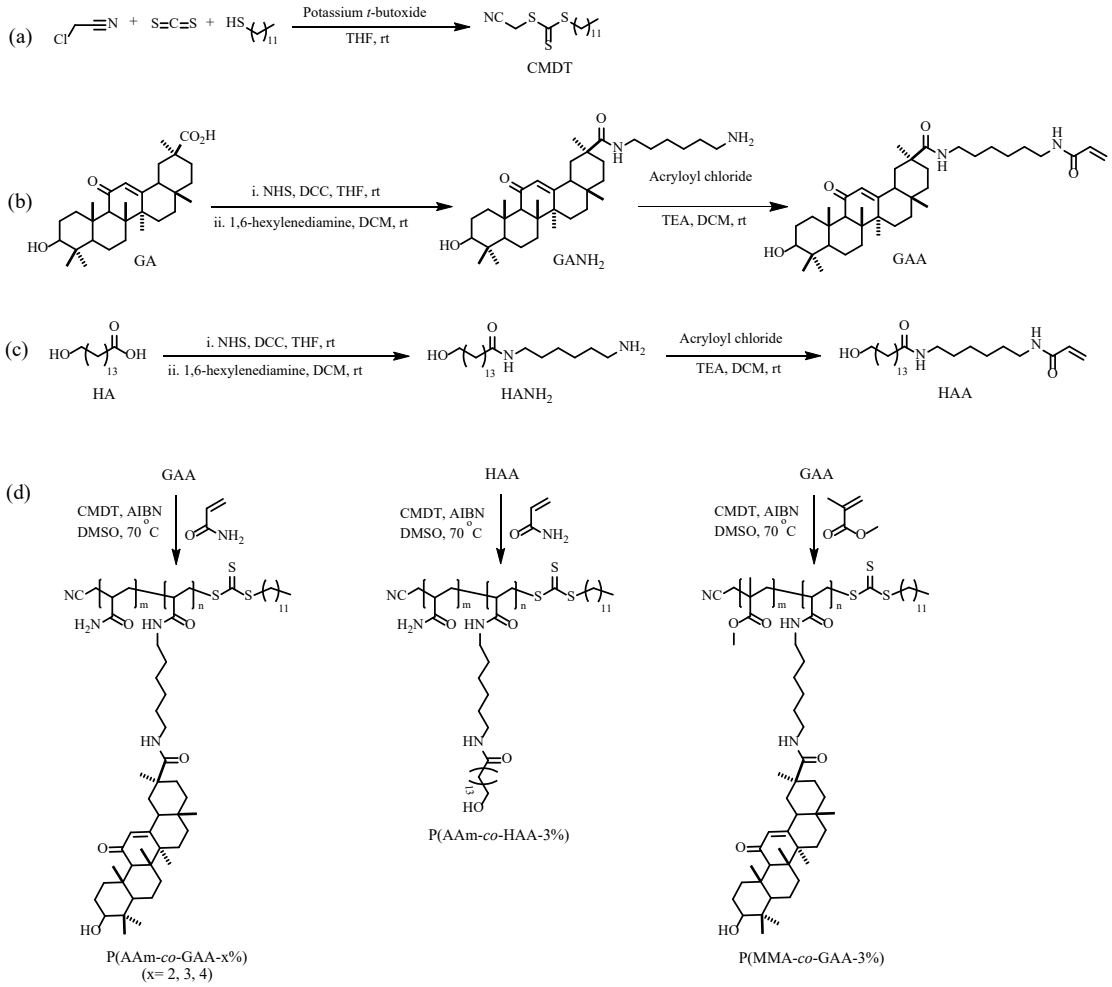

Scheme S1. Synthetic route of copolymers of **P(AAm-*co*-GAA-x%)** (x = 2, 3, 4), **P(AAm-*co*-HAA-3%)**, and **P(MMA-*co*-GAA-3%).**

Synthesis of raft agent CMDT. 1-Dodecanethiol (1.20 mL, 5.04 mmol) and potassium *tert*-butoxide (566 mg, 5.04 mmol) were dissolved in 10 mL THF. After stirring at room temperature for 15 min, carbon disulfide (0.61 mL, 10.08 mmol) was added and stirred for 30 min. Then chloroacetonitrile (0.32 mL, 5.04 mmol) was added and the solution was stirred at room temperature for another 24 h. The resultant solution was evaporated to remove THF and re-dissolved by ethyl acetate. After washing with water, the organic layer was dried by anhydrous Na_2SO_4 and evaporated under reduced pressure. The crude was further purified by chromatography (hexane: ethyl acetate = 80:1, v/v) to afford **CMDT** as a yellow powder (1.55 g, yield 97%). HRMS-ESI (+): m/z calcd for $C_{15}H_{27}NS_3$: 317.1306, found: 318.1382 $[M+H]^+$; ^{1}H NMR (400 MHz, $CDCl_3$, ppm): δ 4.15 (s, 2H, -SCH_2CN), 3.41 (t, 2H, J = 6.96 Hz, -$CH_2C\underline{H_2}S(C=S)S$), 1.72 (m, 2H, -$C\underline{H_2}CH_2S(C=S)S$), 1.5-1.2 (m, 18H, $CH_3(C\underline{H_2})_9CH_2$-), 0.88 (t, 3H, J = 6.64 Hz, $C\underline{H_3}(CH_2)_9CH_2$-); ^{13}C NMR (100 MHz, $CDCl_3$, ppm): δ 218.8, 114.8, 38.0, 31.9, 29.6, 29.5, 29.4, 29.3, 29.1, 28.9, 27.8, 22.7, 21.4, 14.1.

Synthesis of $GANH_2$. To a solution of **GA** (4.00 g, 8.50 mmol) and *N*-hydroxysuccinimide (1.27 g, 11.05 mmol) in 30 mL dry THF, N,N'-dicyclohexylcarbodiimide (2.28 g, 11.05 mmol) in 10 mL dry THF was added dropwise at ice bath. The mixture was stirred at room temperature for 12 h and the precipitates was removed by filtration. The resultant solution was evaporated to remove

THF and re-dissolved by ethyl acetate. After washing with water, the organic layer was dried by anhydrous Na_2SO_4 and evaporated under reduced pressure to afford intermediate GA active ester. This intermediate was dissolved by 50 mL dichloromethane (DCM), and then added dropwise to a DCM solution (150 mL) of 1,6-hexylenediamine (10 g, 86.06 mmol) at room temperature. After stirring for 18 h, the solvent was removed and the crude was re-dissolved by ethyl acetate, washed with water, dried by anhydrous Na_2SO_4, and evaporated under reduced pressure. The crude product was further purified by chromatography (dichloromethane: methanol = 2:1, v/v) to afford **$GANH_2$** as a white powder (1.40 g, yield 29%). ESI-MS (+): m/z 569 $[M+H]^+$; ^{1}H NMR (400 MHz, $CDCl_3$, ppm): δ 5.75 (t, 1H, J = 5.48 Hz, O=C-N$\underline{H}$CH$_2$-), 5.64 (s, 1H, 12-H), 3.17-3.34 (m, 3H, O=C-NHC$\underline{H}_2$-, 3-H), 2.70 (t, 2H, J = 6.84 Hz, $NH_2C\underline{H}_2CH_2$-), 1.36, 1.12, 0.99, 0.80, 0.79 (s, 7 × 3H, 7 × CH_3); ^{13}C NMR (100 MHz, $CDCl_3$, ppm): δ 200.3, 175.6, 169.5, 128.4, 78.7, 61.9, 55.0, 48.2, 45.4, 43.6, 43.3, 41.9, 41.8, 39.3, 39.2, 37.5, 37.1, 33.0, 32.8, 31.9, 31.5, 29.7, 28.5, 28.1, 27.3, 26.6, 26.5, 26.4, 26.3, 23.4, 18.7, 17.5, 16.4, 15.6.

Synthesis of GAA. To a solution of **$GANH_2$** (1.40 g, 2.46 mmol) and triethylamine (0.34 mL, 2.46 mmol) in DCM (60 mL), acryloyl chloride (0.24 mL, 2.95 mmol) in DCM (10 mL) was added dropwise at ice bath. The mixture was stirred at room temperature for 6 h and then the resultant solution was evaporated to remove DCM. The crude was re-dissolved by ethyl acetate, washed with water, and dried by anhydrous Na_2SO_4. After removing the solvent, the crude further was purified by chromatography (dichloromethane: methanol = 10:1, v/v) to afford **GAA** as a white powder (1.34 g, yield 87%). HRMS-ESI (+): m/z calcd for $C_{39}H_{62}N_2O_4$: 622.4710, found: 623.4786 $[M+H]^+$; ^{1}H NMR (400 MHz, $CDCl_3$, ppm): δ 6.29 (m, 1H, CONH), 6.25 (d, 1H, J = 16.92 Hz, -CH=C$\underline{H}_2$), 6.15 (q, 1H, J_1= 18.92 Hz, J_2 = 9.96 Hz, -C$\underline{H}$=CH$_2$), 5.73 (m, 1H, CONH), 5.61 (s, 1H, 12-H), 5.59 (d, 1H, J = 9.96 Hz, -CH=C$\underline{H}_2$), 3.14-3.33 (m, 5H, -C=C-CO-NHC$\underline{H}_2$, C-CO-NHC$\underline{H}_2$, 3-H), 1.37, 1.12, 1.10, 1.00, 0.80 (s, 7 × 3H, 7×CH_3); ^{13}C NMR (100 MHz, $CDCl_3$, ppm): δ 200.3, 175.7, 169.7, 165.7, 131.2, 128.2, 125.9, 78.7, 61.9, 55.0, 53.4, 48.4, 45.5, 43.6, 43.3, 42.2, 39.2, 39.1, 38.9, 38.8, 37.4, 37.1, 32.8, 32.0, 31.4, 31.2, 29.7, 29.6, 29.4, 28.5, 28.1, 27.3, 26.5, 26.4, 26.1, 25.9, 23.3, 18.7, 17.5, 16.4, 15.6.

Synthesis of $HANH_2$. To a solution of **HA** (2.00 g, 7.74 mmol) and *N*-hydroxysuccinimide (1.20 g, 10.43 mmol) in 40 mL dry THF, *N,N*'-dicyclohexylcarbodiimide (2.08 g, 10.08 mmol) in 20 mL dry THF was added dropwise at ice bath. The mixture was stirred at room temperature for 10 h and the precipitates was removed by filtration. The resultant solution was evaporated to remove THF and re-dissolved by ethyl acetate. After washing with water, the organic layer was dried by anhydrous Na_2SO_4 and evaporated under reduced pressure to afford active ester intermediate. This intermediate was dissolved by 200 mL dichloromethane (DCM), and then added dropwise to a DCM solution (250 mL) of 1,6-hexylenediamine (18 g, 154.89 mmol) at room temperature. After stirring for 18 h, the solvent was removed and the crude was re-dissolved by ethyl acetate, washed with water, dried by anhydrous Na_2SO_4, and evaporated under reduced pressure. The crude product was purified by chromatography (dichloromethane: methanol = 2:1, v/v) to afford **$HANH_2$** as a white powder (1.11 g, yield 40%). HRMS-ESI (+): m/z calcd for $C_{21}H_{44}N_2O_2$: 356.3403, found: 357.3491 $[M+H]^+$; ^{1}H NMR (400 MHz, $CDCl_3$, ppm): δ 5.43 (s, 1H, O=C-N$\underline{H}$-), 3.63 (t, 2H, J = 6.64 Hz, OH-C$\underline{H}_2$-), 3.21-3.26 (m, 2H, O=C-NHC$\underline{H}_2$-), 2.68 (t, 2H, J = 6.80 Hz, $NH_2C\underline{H}_2CH_2$-), 2.14 (t, 2H, J = 7.40 Hz, O=C-C$\underline{H}_2$-); ^{13}C NMR (100 MHz, $CDCl_3$, ppm): δ 173.2, 63.1, 37.1, 33.8, 33.0, 29.8, 29.7, 29.6, 29.5, 29.4, 26.9, 26.7, 26.0, 25.9.

Synthesis of HAA. To a solution of **$HANH_2$** (530 mg, 1.49 mmol) and triethylamine (0.27 mL, 1.93 mmol) in DCM (120 mL), acryloyl chloride (0.12 mL, 1.49 mmol) in DCM (5 mL) was added dropwise at ice bath. The mixture was stirred at room temperature for 6 h and then the resultant solution was evaporated to remove DCM. The crude was re-dissolved by ethyl acetate, washed with water, and dried by anhydrous Na_2SO_4. After removing the solvent, the crude further was purified by chromatography (dichloromethane: methanol = 10:1, v/v) to afford **HAA** as a white powder (0.35 g, yield 57%). HRMS-ESI (+): m/z calcd for $C_{24}H_{46}N_2O_3$: 410.3508, found: 411.3605 $[M+H]^+$; ^{1}H NMR (400 MHz, d_6-DMSO, ppm): δ 8.04, 7.70 (s, 2 × 1H, -CON*H*), 6.19 (q, 1H, J_1= 17.08 Hz, J_2 = 10.04 Hz, -C*H*=CH_2), 6.03 (q, 1H, J_1= 17.08 Hz, J_2 = 2.32 Hz, -CH=C*H*$_2$), 5.54 (q, 1H, J_1= 10.04 Hz, J_2 = 2.32 Hz, -CH=C*H*$_2$), 3.36 (t, 2H, J = 6.48 Hz, OH-C*H*$_2$-), 3.09, 3.00 (m, 2 × 2H, -CONHC*H*$_2$-), 2.02 (t, 2H, J = 7.28 Hz, -C*H*$_2$-CONHCH$_2$-); ^{13}C NMR (100 MHz, $CDCl_3$/CD_3OD, v/v = 15:1, ppm): δ 174.3, 166.4, 130.8, 126.3, 62.7, 39.0, 36.7, 32.6, 29.6, 29.5, 29.3, 29.2, 29.0, 25.9, 25.8.

Polymerization of P(AAm-*co*-GAA-x%) (x = 2, 3, 4), P(AAm-*co*-HAA-3%), and P(MMA-*co*-GAA-3%). Copolymerization was conducted in DMSO at 70 °C with a [comonomers]/[CMDT]/[AIBN] = 340:1:0.2. For example, **GAA** (80 mg, 0.13 mmol), AAm (445 mg, 6.27 mmol), CMDT (6.0 mg, 0.019 mmol) and AIBN (0.6 mg, 0.004 mmol) were dissolved in 1.5 mL DMSO in Schlenk tube, and the mixture was purged with Ar for 40 min prior to its immersion in a preheated oil bath. The copolymerization was allowed to proceed for 20 h before being quenched by immersion into ice water. After that, 5 mL DMSO was added to dissolve the copolymer, and the precipitate was collected after pouring the mixture into 200 mL methanol. The copolymer was dried in vacuo to yield 466 mg of P(AAm-*co*-GAA-2%). The polymers with different GA contents, P(AAm-*co*-HAA-3%), and P(MMA-*co*-GAA-3%) were synthesized using the similar method.

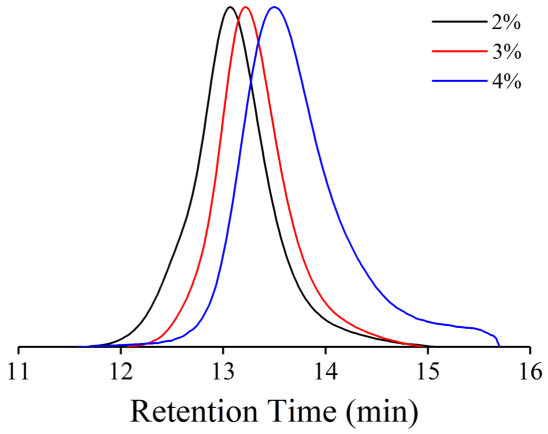

Fig. S1. SEC spectra of P(AAm-*co*-GAA-x%) (x = 2, 3, 4) with refractometer as detector (DMSO as eluent, dextran standards for molecular weight calibration). The right shoulder peak of P(AAm-*co*-GAA-4%) was mainly due to the formation of trace oligomers.

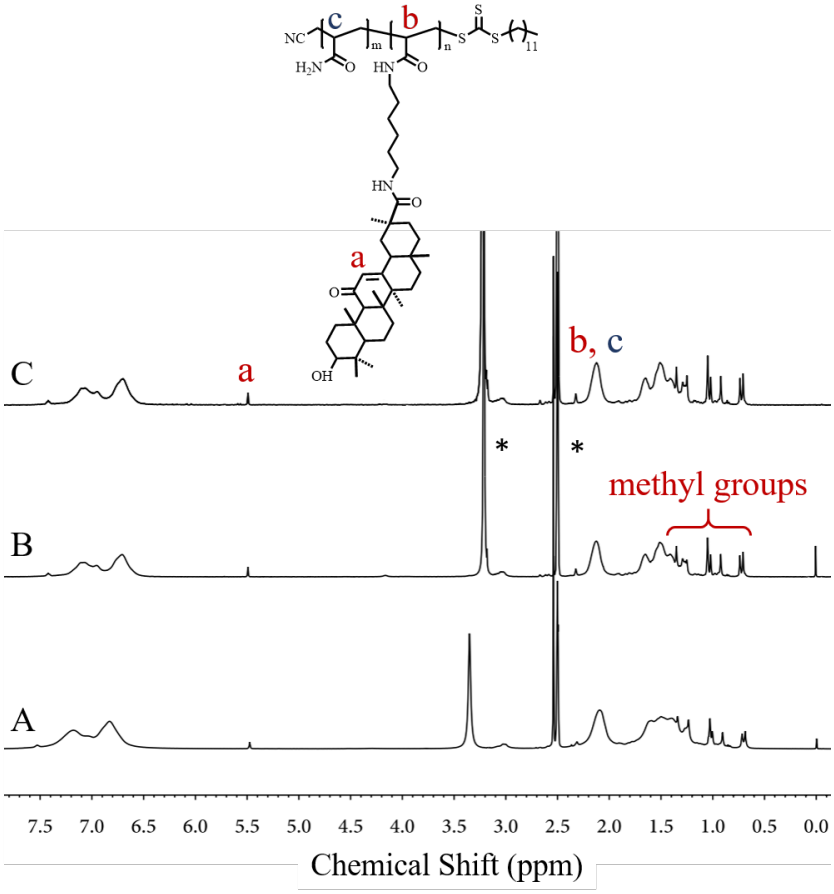

Fig. S2. ^{1}H NMR spectra (400 MHz, d_6-DMSO) of P(AAm-*co*-GAA-x%) in the molar fraction of GAA (A) 2%, (B) 3%, and (C) 4%. "*" means DMSO and water.

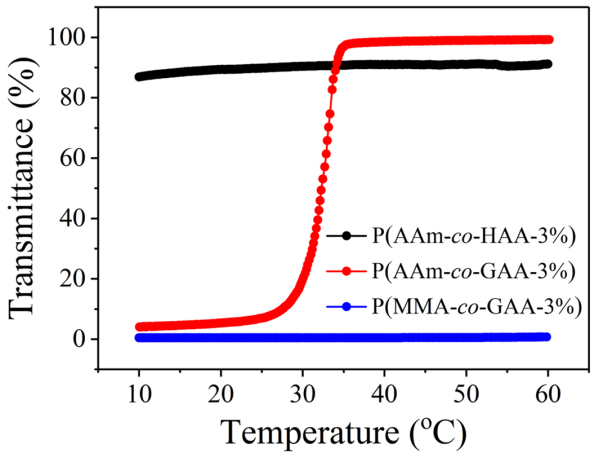

Fig. S3. Transmittance of the aqueous solutions of P(AAm-*co*-GAA-3%), P(AAm-*co*-HAA-3%), and P(MMA-*co*-GAA-3%) as a function of temperature at a wavelength of 450 nm and a cooling rate of 1.0 °C/min at the concentration of 15 mg/mL.

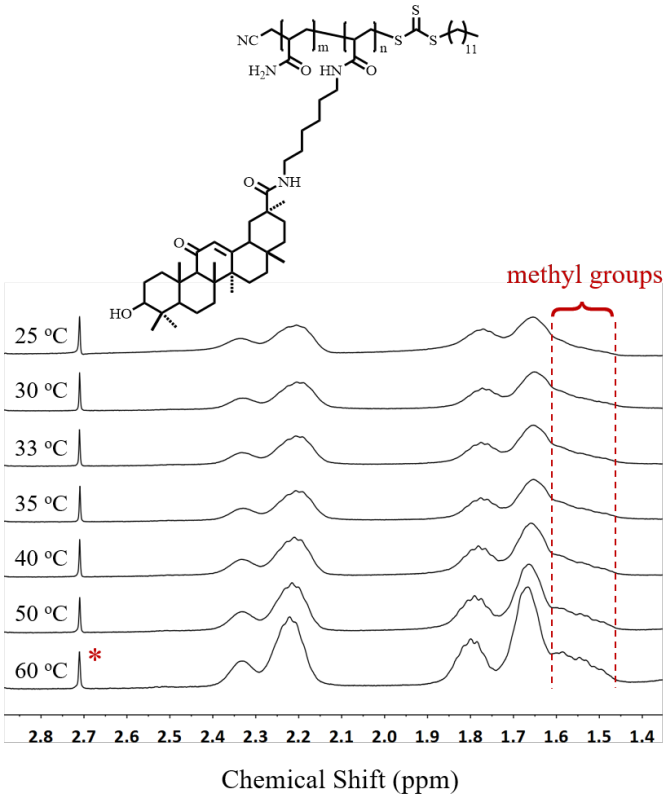

Fig. S4. Temperature-dependent ^{1}H NMR spectra of P(AAm-*co*-GAA-3%) in D_2O upon cooling from 60 to 25 °C at the concentration of 15 mg/mL. "*" means DMSO.

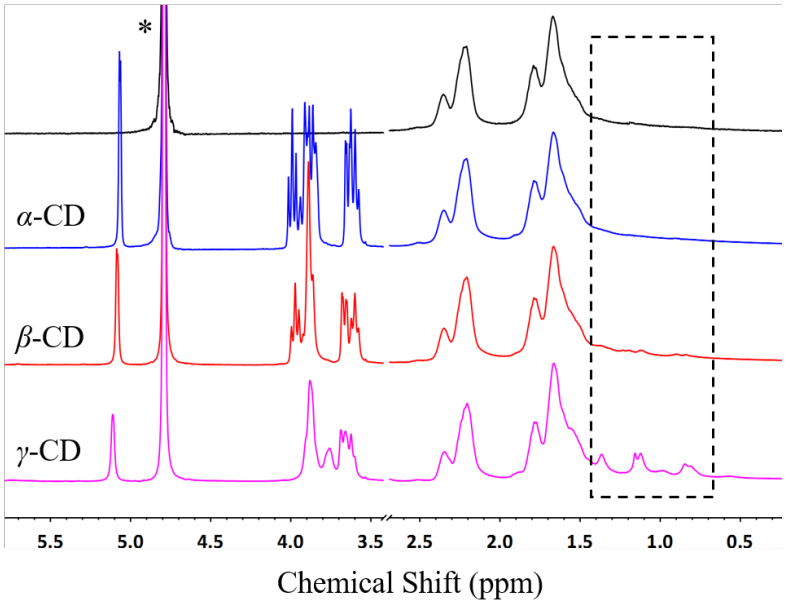

Fig. S5. ^{1}H NMR spectra of P(AAm-*co*-GAA-3%) in D_2O at the concentration of 15 mg/mL upon addition of *α*-, *β*-, or *γ*-CD, respectively ([GA]/[CD] = 1:1). "*" means D_2O.

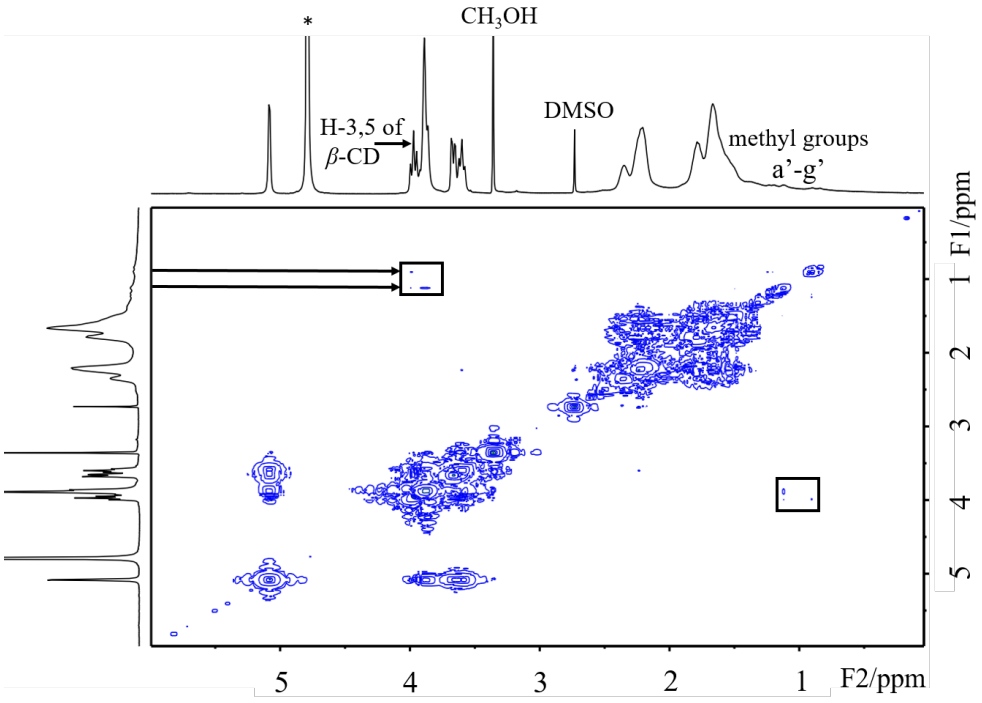

Fig. S6. 2D NOESY ^{1}H NMR spectrum of P(AAm-*co*-GAA-3%) with *β*-CD in D_2O (600 MHz). "*" means D_2O.

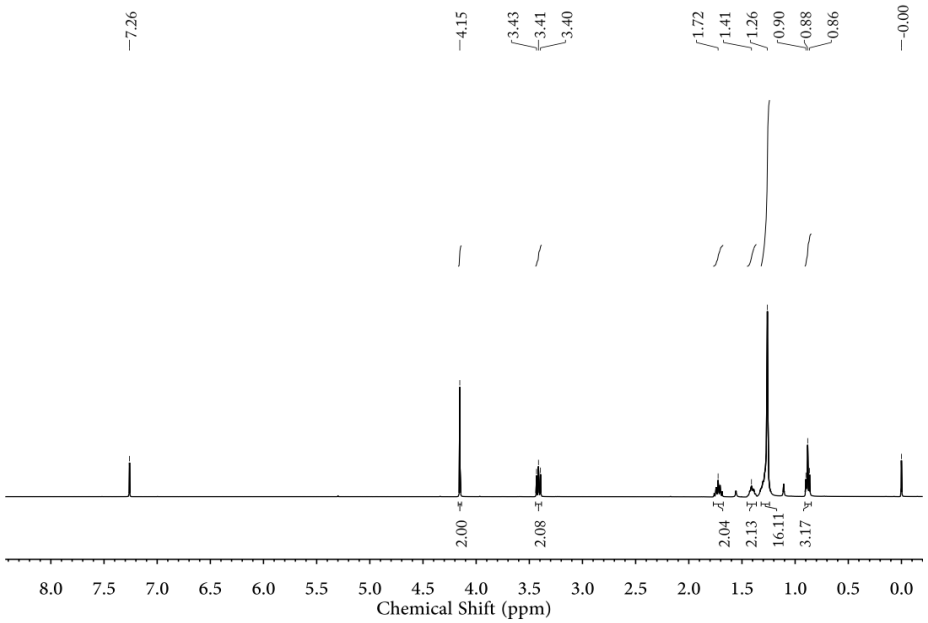

Fig. S7. ^{1}H NMR spectrum of **CMDT** (400 MHz, $CDCl_3$)

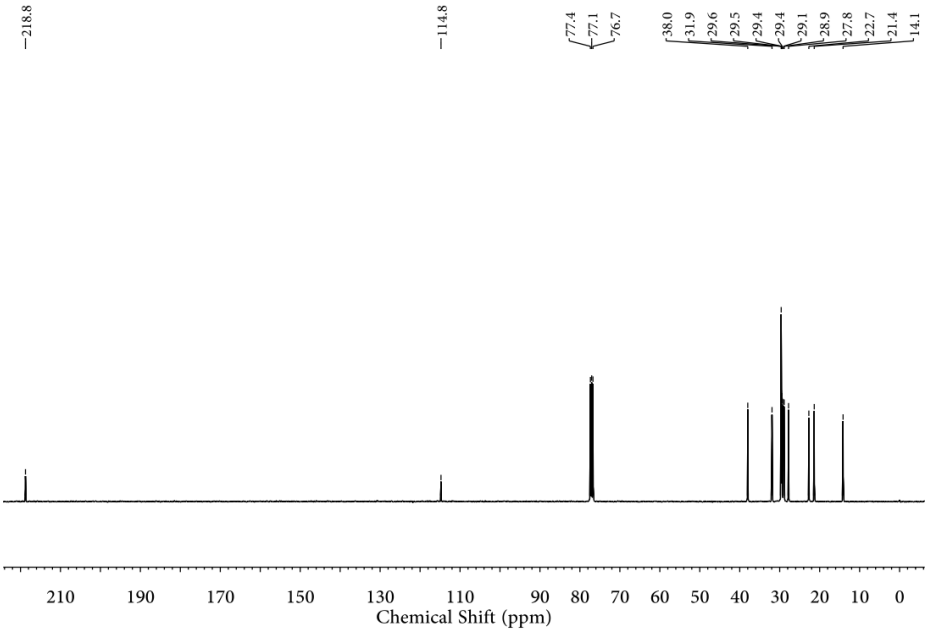

Fig. S8. ^{13}C NMR spectrum of **CMDT** (100 MHz, $CDCl_3$)

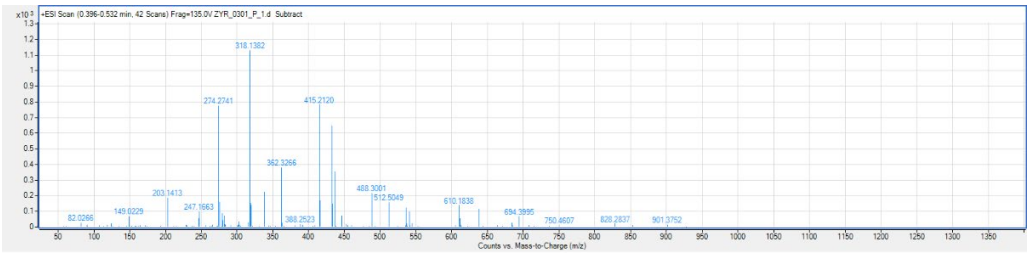

Fig. S9. HRMS-ESI (+) spectrum of **CMDT**

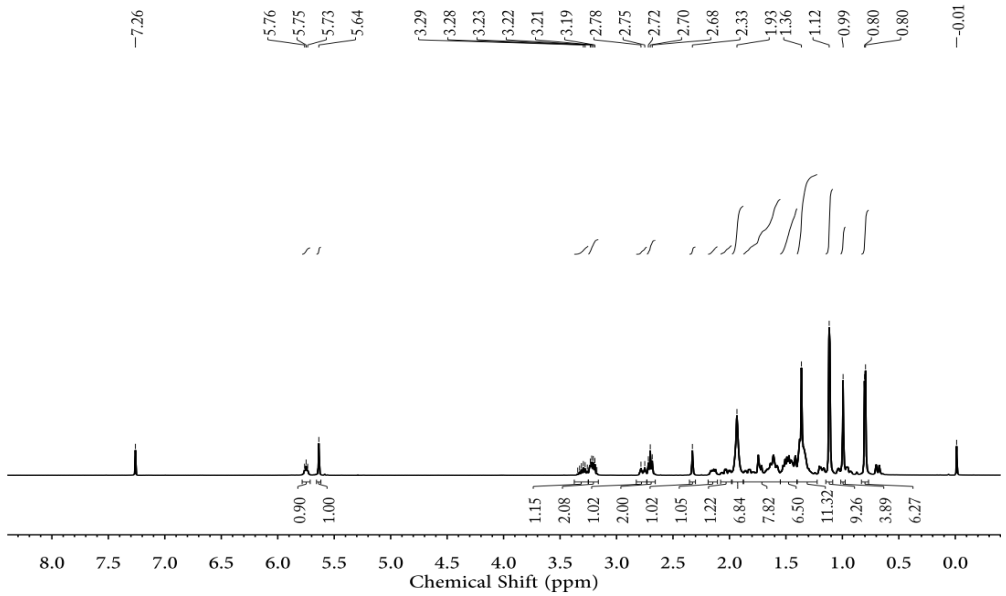

Fig. S10. ^{1}H NMR spectrum of **GANH$_2$** (400 MHz, $CDCl_3$)

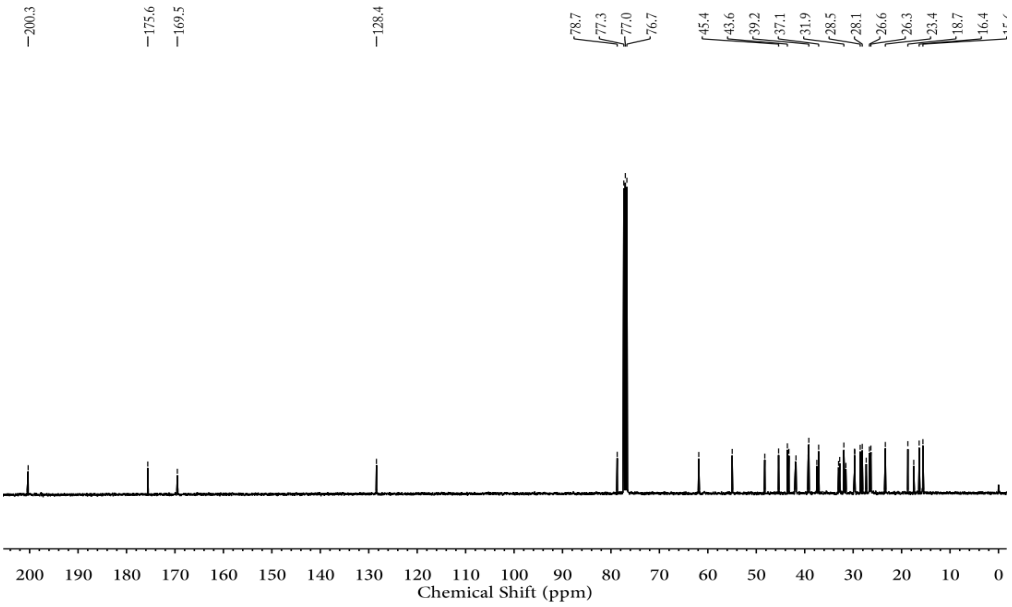

Fig. S11. ^{13}C NMR spectrum of **GANH$_2$** (100 MHz, $CDCl_3$)

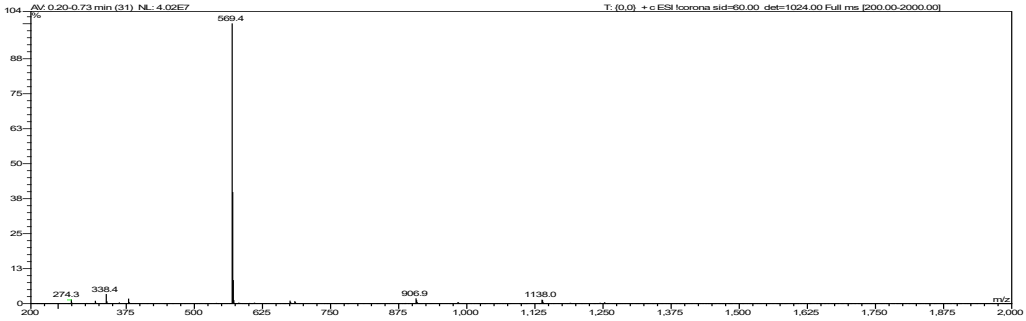

Fig. S12. ESI-MS (+) spectrum of **GANH$_2$**

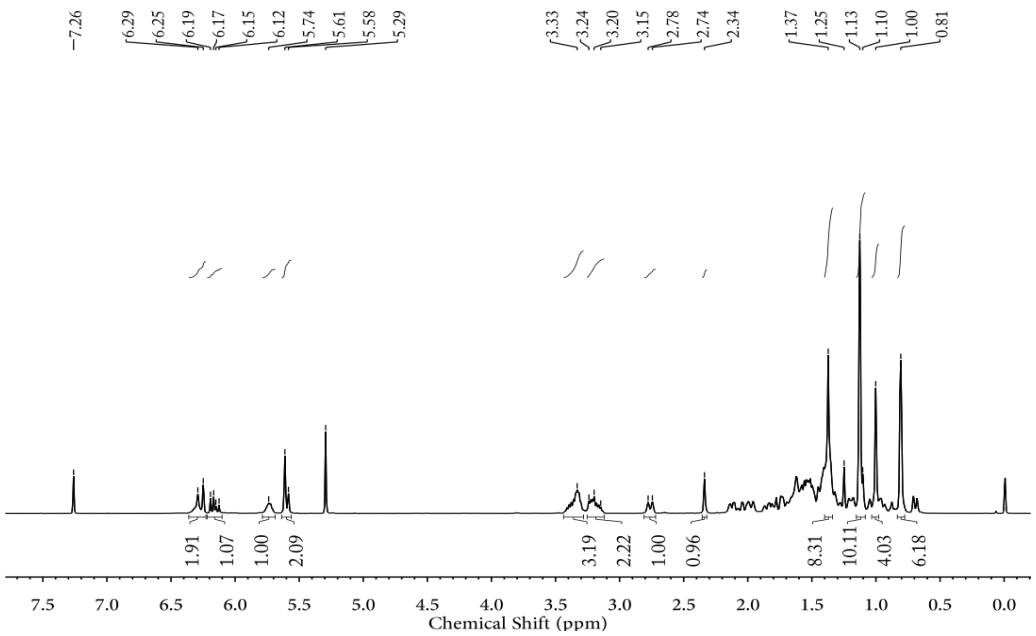

Fig. S13. ^{1}H NMR spectrum of **GAA** (400 MHz, $CDCl_3$)

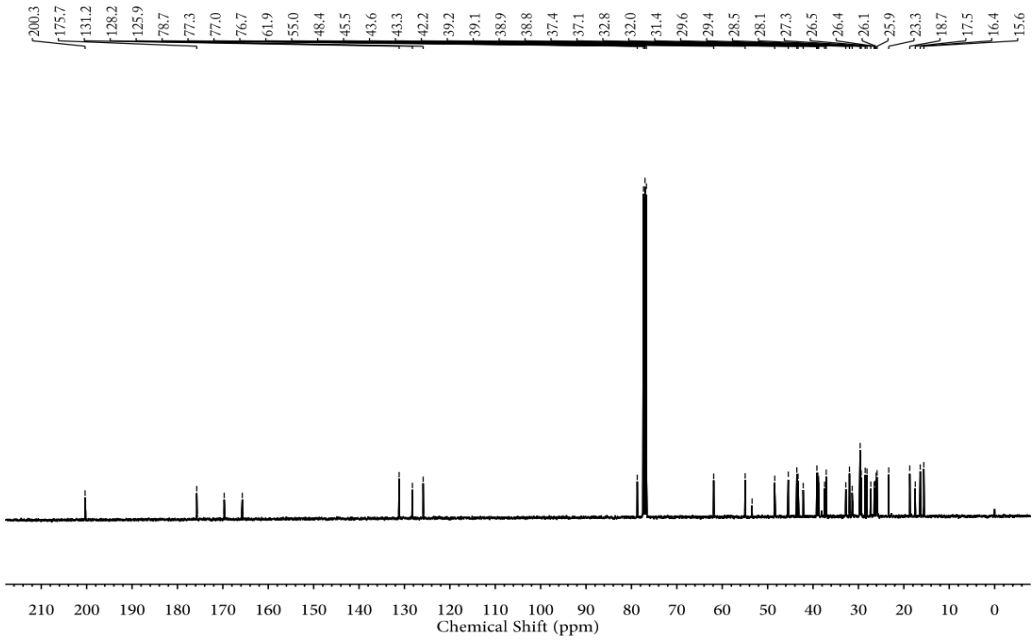

Fig. S14. ^{13}C NMR spectrum of **GAA** (100 MHz, $CDCl_3$)

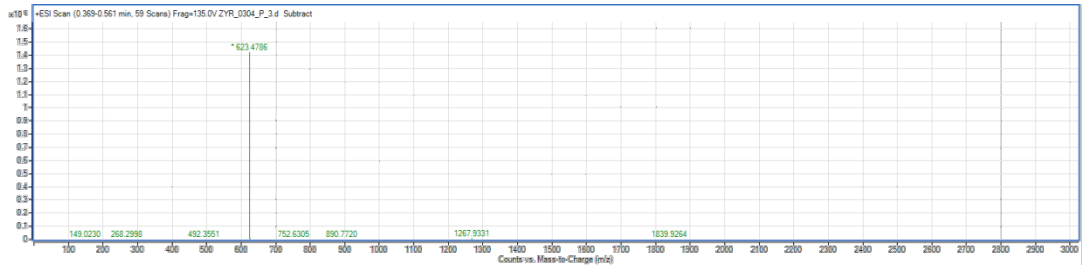

Fig. S15. HRMS-ESI (+) spectrum of **GAA**

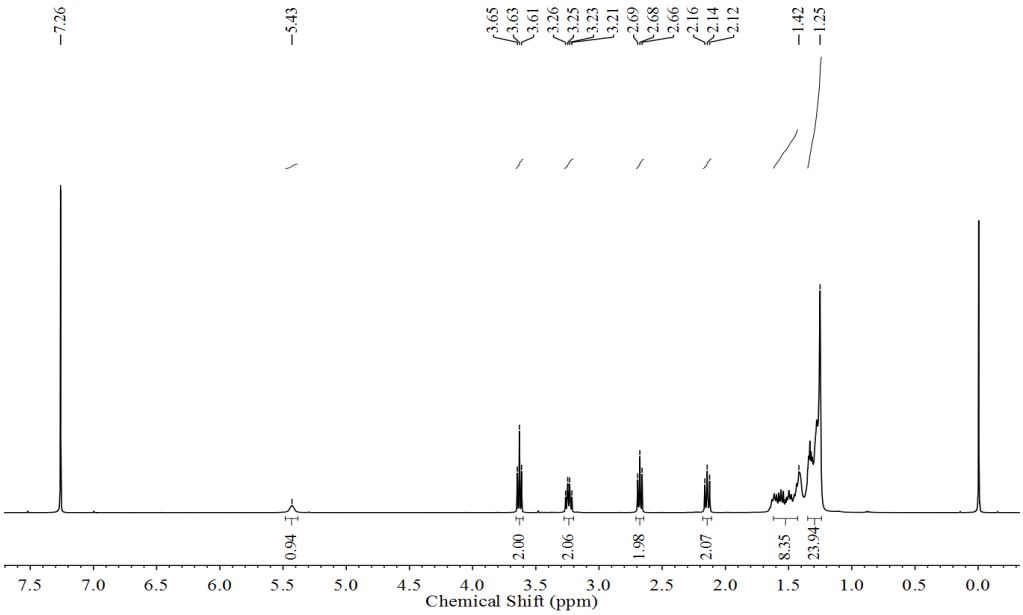

Fig. S16. ^{1}H NMR spectrum of **HANH$_2$** (400 MHz, $CDCl_3$)

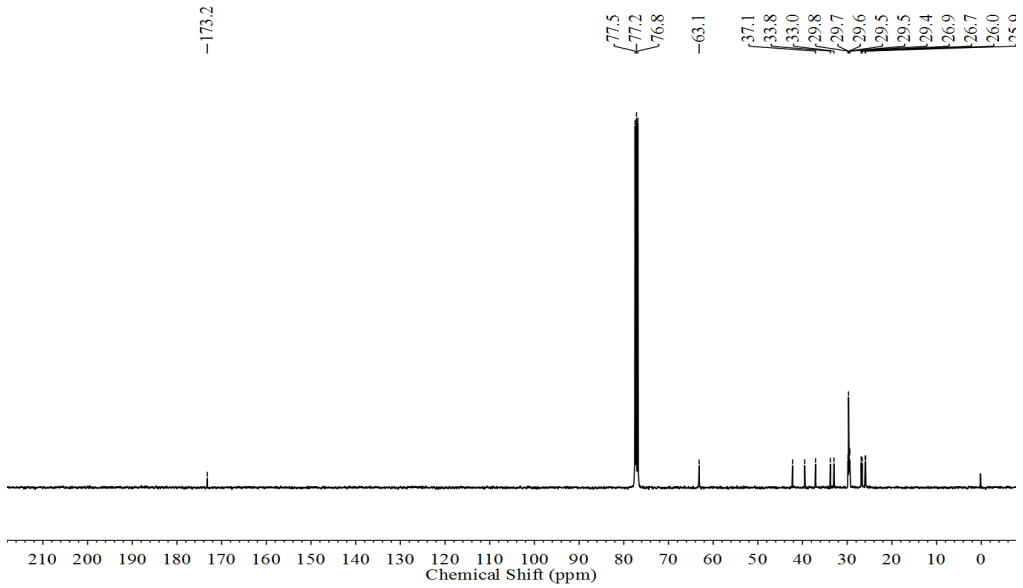

Fig. S17. ^{13}C NMR spectrum of **HANH$_2$** (100 MHz, $CDCl_3$)

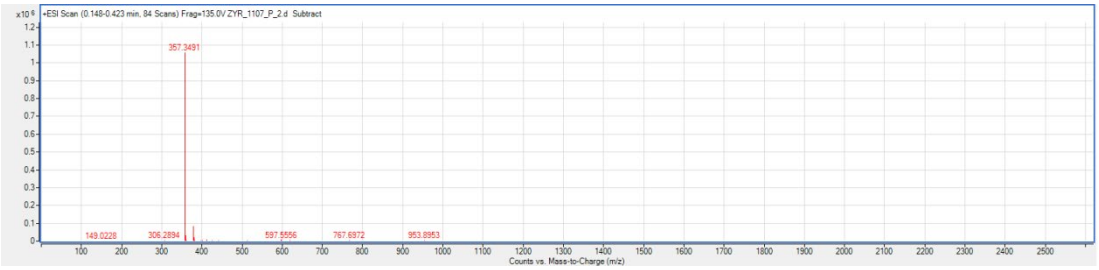

Fig. S18. HRMS-ESI (+) spectrum of **HANH$_2$**

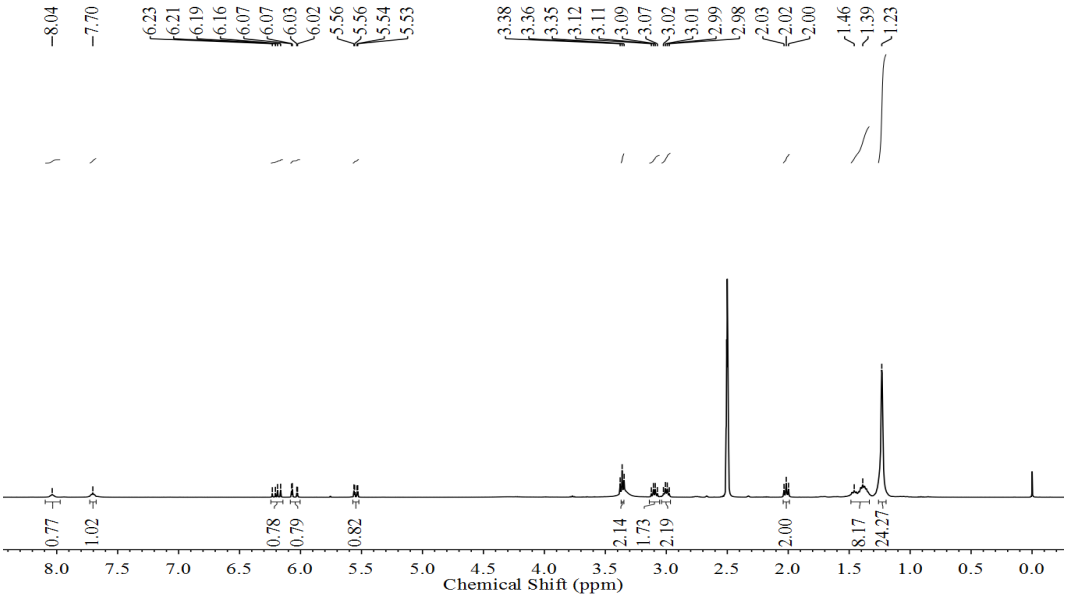

Fig. S19. ^{1}H NMR spectrum of **HAA** (400 MHz, d_6-DMSO)

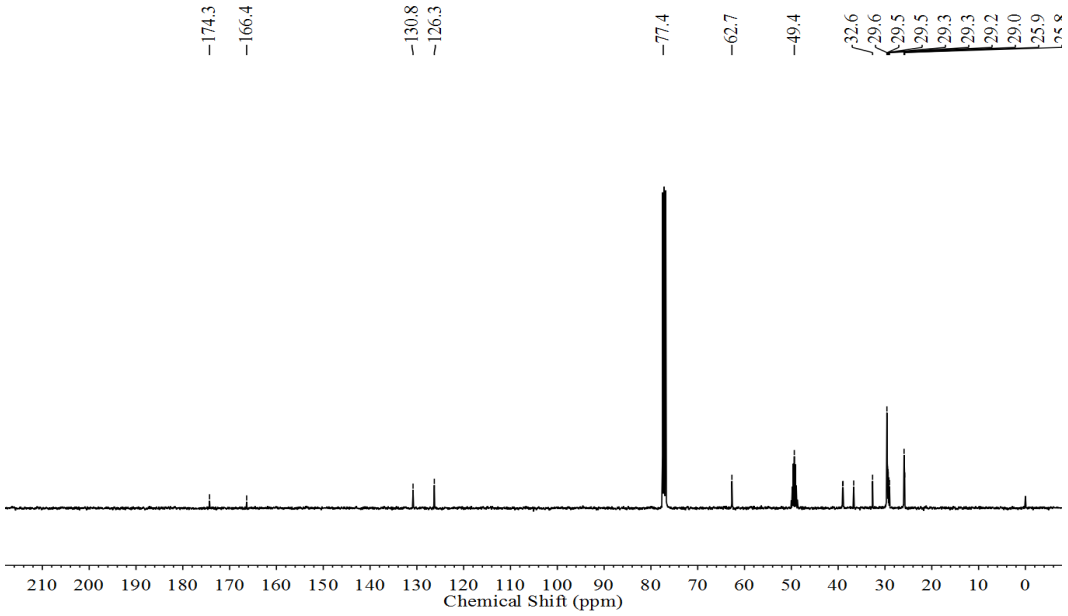

Fig. S20. ^{13}C NMR spectrum of **HAA** (100 MHz, $CDCl_3/CD_3OD$, v/v = 15:1)

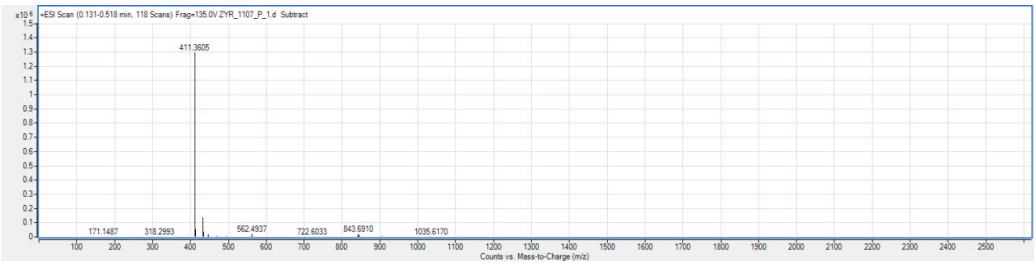

Fig. S21. HRMS-ESI (+) spectrum of **HAA**

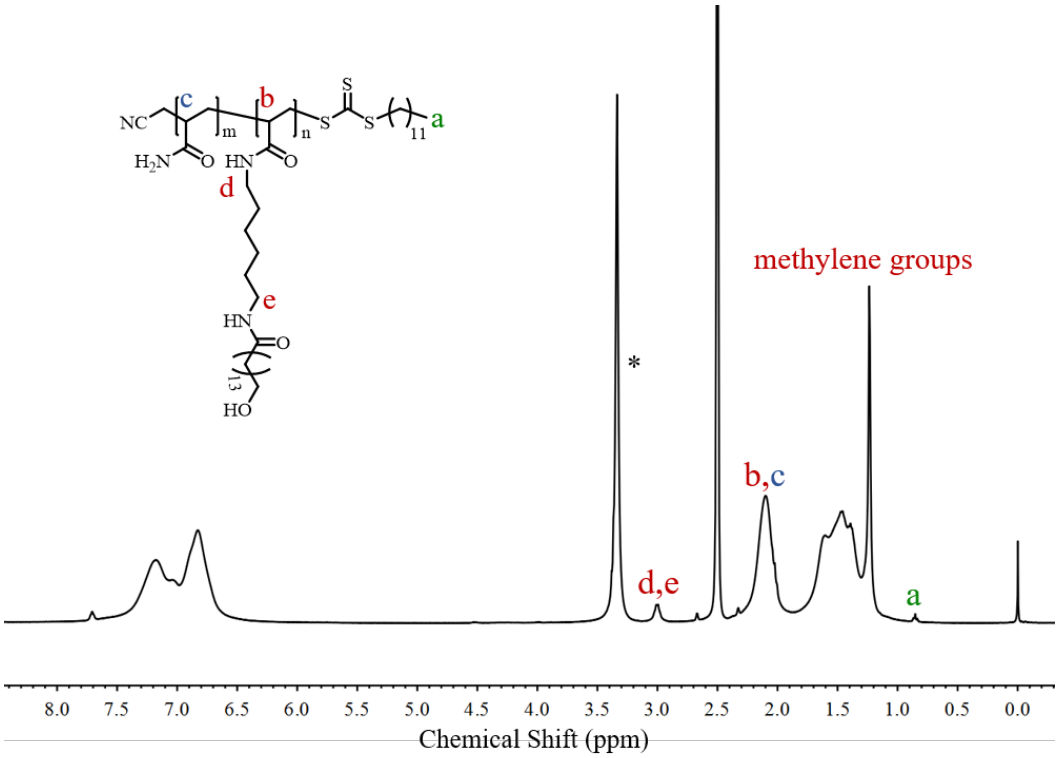

Fig. S22. ^{1}H NMR spectrum of copolymer P(AAm-*co*-HAA-3%) (400 MHz, d_6-DMSO). "*" means water.

The content of HAA units in P(AAm-*co*-HAA-3%) was calculated from the proton integration ratio between the peaks at 2.98-3.02 ppm (H_d and H_e) versus backone protons at 2.10 ppm (H_b and H_c). In addition, the molar mass of P(AAm-*co*-HAA-3%) was determined by the integral values of protons in HAA (H_d and H_e), protons in AAm (H_c), and protons of end groups in the main chain (H_a, 0.85 ppm). The molar mass was calculated as follows:

$$\text{Molar mass} = \frac{3Int_{d,e}}{4Int_a} \times M_{HAA} + \frac{3\left(Int_{b,c} - {Int_{d,e}}/{4}\right)}{Int_a} \times M_{AAm} + M_{CMDT}$$

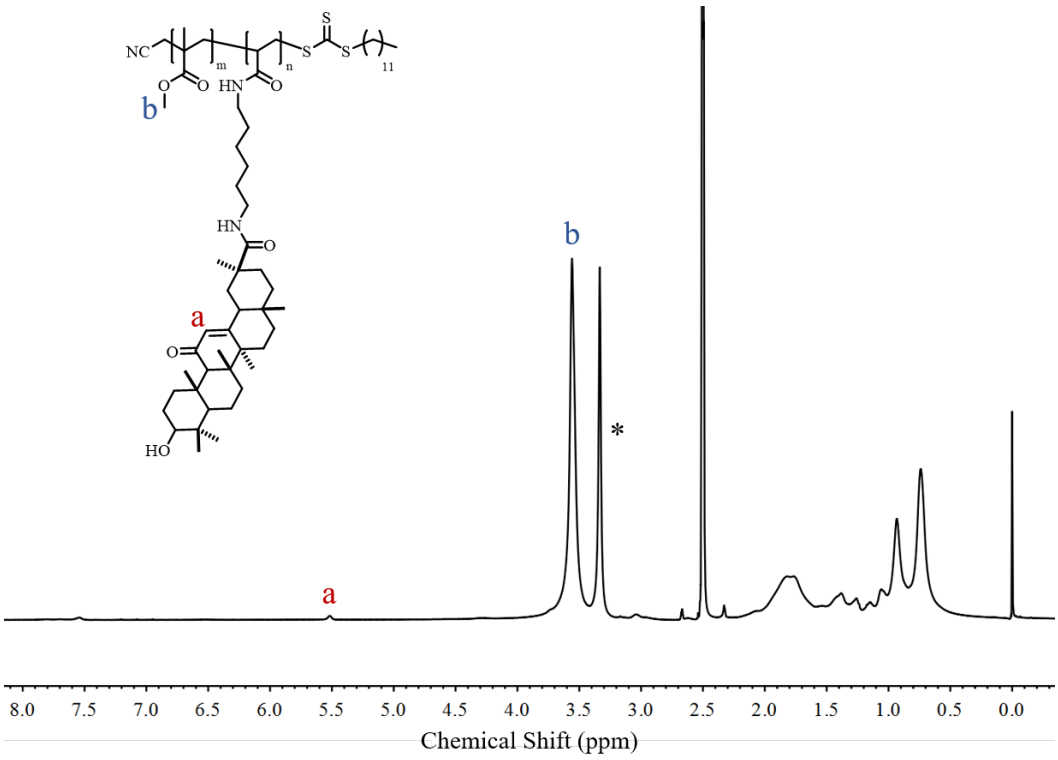

Fig. S23. ^{1}H NMR spectrum of copolymer P(MMA-*co*-GAA-3%) (400 MHz, d_6-DMSO). "*" means water.

The content of GAA units in P(MMA-*co*-GAA-3%) was calculated from the proton integration ratio between the peak at 5.52 ppm (H_a) versus methyl protons at 3.56 ppm (H_b).

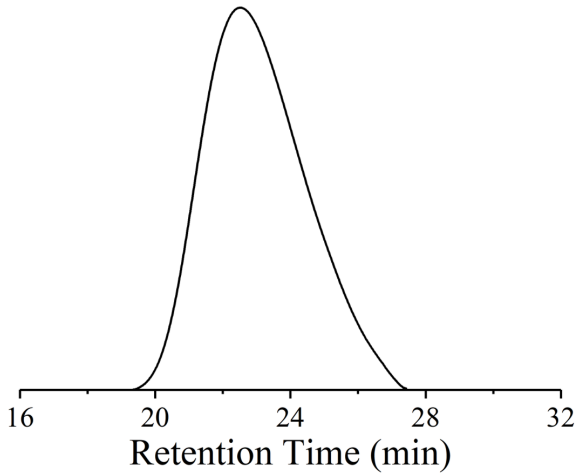

Fig. S24. SEC spectrum of P(MMA-c*o*-GAA-3%) with refractometer as detector (DMAC as eluent, polystyrene standards for molecular weight calibration).